Thermally enhanced signal strength and SNR improvement of photoacoustic radar module

Wei Wang and Andreas Mandelis*

Center for Advanced Diffusion Wave Technologies (CADIFT), Dept. of Mechanical and Industrial Engineering, University of Toronto, Toronto M5S3G8, Canada
**mandelis@mie.utoronto.ca*

Abstract: A thermally enhanced method for improving photoacoustic imaging depth and signal-to-noise (SNR) ratio is presented in this paper. Experimental results showed that the maximum imaging depth increased by 20% through raising the temperature of absorbing biotissues (*ex-vivo* beef muscle) uniformly from 37 to 43°C, and the SNR was increased by 8%. The parameters making up the Gruneisen constant were investigated experimentally and theoretically. The studies showed that the Gruneisen constant of biotissues increases with temperature, and the results were found to be consistent with the photoacousitc radar theory.

OCIS codes: (170.5120) Photoacoustic imaging; (170.3880) Medical and biological imaging.

References and links

1. J. L. Kovar, M. A. Simpson, A. Schutz-Geschwender, and D. M. Olive, "A systematic approach to the development of fluorescent contrast agents for optical imaging of mouse cancer models," Anal. Biochem. **367**(1), 1–12 (2007).
2. B. Lashkari and A. Mandelis, "Comparison between pulsed laser and frequency-domain photoacoustic modalities: signal-to-noise ratio, contrast, resolution, and maximum depth detectivity," Rev. Sci. Instrum. **82**(9), 094903 (2011).
3. G. Ku and L. V. Wang, "Deeply penetrating photoacoustic tomography in biological tissues enhanced with an optical contrast agent," Opt. Lett. **30**(5), 507–509 (2005).
4. R. Alwi, S. Telenkov, A. Mandelis, T. Leshuk, F. Gu, S. Oladepo, and K. Michaelian, "Silica-coated super paramagnetic iron oxide nanoparticles (SPION) as biocompatible contrast agent in biomedical photoacoustics," Biomed. Opt. Express **3**(10), 2500–2509 (2012).
5. G. Kelly, "Body temperature variability (part 1): a review of the history of body temperature and its variability due to site selection, biological rhythms, fitness, and aging," Altern. Med. Rev. **11**(4), 278–293 (2006).
6. P. A. Mackowiak and G. Worden, "Carl Reinhold August Wunderlich and the evolution of clinical thermometry," Clin. Infect. Dis. **18**(3), 458–467 (1994).
7. M. Sund-Levander, C. Forsberg, and L. K. Wahren, "Normal oral, rectal, tympanic and axillary body temperature in adult men and women: a systematic literature review," Scand. J. Caring Sci. **16**(2), 122–128 (2002).
8. H. I. Robins, W. H. Dennis, A. J. Neville, L. M. Shecterle, P. A. Martin, J. Grossman, T. E. Davis, S. R. Neville, W. K. Gillis, and B. F. Rusy, "A nontoxic system for 41.8 degrees C whole-body hyperthermia: results of a Phase I study using a radiant heat device," Cancer Res. **45**(8), 3937–3944 (1985).
9. L. F. Fajardo, "Pathological effects of hyperthermia in normal tissues," Cancer Res. **44**(10 Suppl), 4826s–4835s (1984).
10. J. van der Zee, "Heating the patient: a promising approach?" Ann. Oncol. **13**(8), 1173–1184 (2002).
11. P. Sminia, J. van der Zee, J. Wondergem, and J. Haveman, "Effect of hyperthermia on the central nervous system: a review," Int. J. Hyperthermia **10**(1), 1–30 (1994).
12. H. Siekmann, "Recommended maximum temperatures for touchable surfaces," Appl. Ergon. **21**(1), 69–73 (1990).
13. I. V. Larina, K. V. Larin, and R. O. Esenaliev, "Real-time optoacoustic monitoring of temperature in tissues," J. Phys. D Appl. Phys. **38**(15), 2633–2639 (2005).
14. M. Pramanik and L. V. Wang, "Thermoacoustic and photoacoustic sensing of temperature," J. Biomed. Opt. **14**(5), 054024 (2009).
15. W. Wang and A. Mandelis, "Thermally enhanced photoacoustic imaging of biotissues," presented at ICPPP 17th, Suzhou, China, 20–24 Oct. (2013).
16. Y. Fan, A. Mandelis, G. Spirou, and I. A. Vitkin, "Development of a laser photothermoacoustic frequency-swept system for subsurface imaging: theory and experiment," J. Acoust. Soc. Am. **116**(6), 3523–3533 (2004).

#211182 - $15.00 USD Received 9 May 2014; revised 30 Jun 2014; accepted 7 Jul 2014; published 25 Jul 2014

17. V. E. Gusev and A. A. Karabutov, *Laser Optoacoustics* (AIP, 1993).
18. S. A. Telenkov and A. Mandelis, "Fourier-domain biophotoacoustic subsurface depth selective amplitude and phase imaging of turbid phantoms and biological tissue," J. Biomed. Opt. **11**(4), 044006 (2006).
19. E. O. Brigham, *The Fast Fourier Transform and its Applications* (Prentice-Hall, 1988).
20. R. A. Lawrie and D. Ledward, *Lawrie's Meat Science* (Woodhead, 2006).
21. A. M. Pearson and R. B. Young, *Muscle and Meat Biochemistry* (Academic, 1989).
22. B. A. Fricke and B. R. Becker, "Evaluation of thermophysical property models for foods," HVAC and R. Research. **7**(4), 311–330 (2001).
23. Y. Choi and M. R. Okos, "Effects of temperature and composition on the thermal properties of foods," in *Food Engineering and Process Applications: Transport Phenomena,* M. Le Maguer and P. Jelen, ed. (Elsevier, 1986).
24. V. A. Dubinskaya, L. S. Eng, L. B. Rebrow, and V. A. Bykov, "Comparative study of the state of water in various human tissues," Bull. Exp. Biol. Med. **144**(3), 294–297 (2007).
25. J. A. Dean, ed., *Lange's Handbook of Chemistry* (McGraw-Hill, 1973).
26. N. S. Osborne, H. F. Stimson, and D. C. Ginnings, "Measurements of heat capacity and heat of vaporization of water in the range 0° to 100°C," J. Res. Nat. Bur. Stand. (U.S.) **23**(2), 197–260 (1939).
27. S. Temkin, *Elements of Acoustics* (Wiley, 1981).
28. H. J. van Staveren, C. J. M. Moes, J. van Marie, S. A. Prahl, and M. J. van Gemert, "Light scattering in Intralipid-10% in the wavelength range of 400-1100 nm," Appl. Opt. **30**(31), 4507–4514 (1991).

1. Introduction

Photoacoustic (PA) imaging is based on light absorption and detects ultrasound signals generated through non-radiative energy conversion of light and thermoelastic expansion. Near infrared wavelengths exhibit low absorption coefficient and relatively low scattering cross-section in biotissues, so the optical window in the 700 to 900 nm range allows light to penetrate relatively deep [1]. In addition, system parameter optimization, sophisticated signal processing and high laser power can also improve image quality [2]. Furthermore, the PA signal can be enhanced by contrast agents, such as Indocyanine Green (ICG) dye [3] and silica-coated super paramagnetic iron oxide nanoparticles (SPION) [4]. Even though these methods can improve SNR and imaging depth significantly, contrast agents are not without health risks and are, therefore, invasive.

The widely accepted body temperature of a healthy adult is approximately 37°C [5,6]. Normal body temperature changes from person to person and different parts of the human body have different normal temperature. The upper limit of a normal body temperature is 38°C, and the lower limit is 35°C [7]. In summary, the literature indicates that mean normal adult body temperature ranges from 35.5 to 37°C [7].

Studies show that raising the temperature of the whole human body up to 41.8°C for less than an hour is generally safe [8]. With localized heating, most normal tissues such as liver, kidney, and muscles can withstand temperature up to 44°C for 30 minutes [8–10]. However, the central nervous tissue is most sensitive to temperature, and damage was found after exposure to over 42°C for longer than 30 minutes [9,11]. The skin is less sensitive to increased temperature than other tissues, and the recommended maximum contact temperature without burn injuries is 43°C for the maximum time of 8 hour [12]. The safe exposure time of skin is shortened by about 50% for each temperature degree increase up to 50°C, and it sustains no injury when exposed to 60°C for only a few seconds [12].

Temperature can affect PA signals; the signal becomes stronger at higher temperatures [13–15]. This phenomenon has been used for temperature monitoring [14] and imaging improvement [15]. However, a detailed study of the PA signal increase with temperature has not been reported to the best of our knowledge. In this paper, we investigate the details of the temperature dependence of parameters influencing the PA signal, and we present a technique for using heat as a method to increase PA signal strength, signal-to-noise ratio, and PA imaging depth.

#211182 - $15.00 USD Received 9 May 2014; revised 30 Jun 2014; accepted 7 Jul 2014; published 25 Jul 2014

2. Theoretical background

Frequency domain photoacoustics (FDPA) uses modulated continuous wave (CW) laser beams which, upon absorption, generate temperature oscillations in a sample and produce thermoelastic acoustic pressure oscillations.

The response amplitude spectrum $|\tilde{p}(\omega)|$ of the acoustic pressure is generated by the spatially distributed energy source spectrum $\tilde{E}(\omega)$ [J/m^2] in a chromophore and can be described in one dimension by [16–18]:

$$|\tilde{p}(\omega)| \approx \frac{\mu_a \beta c_a^2 e^{-\mu_{ef} z}}{C_p \sqrt{\mu_a^2 c_a^2 + \omega^2}} E_0 = \frac{\mu_a \Gamma e^{-\mu_{ef} z}}{\sqrt{\mu_a^2 c_a^2 + \omega^2}} E_0 \tag{1}$$

where ω [rad/s] represents the angular modulation frequency, μ_a [m^{-1}] is the absorption coefficient, β [°C^{-1}] is the volume thermal expansion coefficient, c_a [m/s] is the speed of sound, μ_{ef} [m^{-1}] is the effective attenuation coefficient, z [m] is the distance, E_0 [J·Hz/m^2] is the frequency modulated light intensity at the surface of the absorber, C_p [J/kg°C] is the specific heat capacity at constant pressure, and $\Gamma = \frac{\beta c_a^{\,2}}{C_p}$ is the Gruneisen parameter. From Eq. (1), we can deduce that the amplitude of the PA signal is proportional to the square of the speed of sound c_a, absorption coefficient μ_a, thermal expansion coefficient β and light intensity E_0, but inversely proportional to the specific heat capacity C_p and ω for $\omega \gg \mu_a c_a$. The phase θ of the pressure spectrum can be derived as:

$$\theta = \tan^{-1}\left(\frac{\omega \cos(\frac{\omega z}{c_a}) + \mu_a c_a \sin(\frac{\omega z}{c_a})}{\omega \sin(\frac{\omega z}{c_a}) - \mu_a c_a \cos(\frac{\omega z}{c_a})} \right) \tag{2}$$

In frequency domain signal processing, the Fourier transforms of the detected s_t and the reference signal r_t are $s(\omega)$ and $r(\omega)$, respectively. In turn, the complex conjugate of the reference signal $r^*(\omega)$ is obtained. After convolution of $r^*(\omega)$ with $s(\omega)$ and inverse Fourier transformation (IFFT), the cross-correlation result $R(t)$ is obtained as follows [19]:

$$R(t) = \frac{1}{2\pi} \int_{-\infty}^{+\infty} s(\omega) \bullet r^*(\omega) e^{i\omega t} d\omega \tag{3}$$

In terms of molecular composition, bio-tissues are a mixture of water, proteins, nucleic acids, lipids, carbohydrates and mineral components [20,21]. A typical composition of beef muscle approximately consists of 75% water, 19% protein, 3% fat, 1% fiber, 1% carbohydrate, and 1% ash [20,21].

Composition-based thermal property prediction methods use composition data for the estimation of the thermal expansion coefficient and the specific heat capacity of biotissues. The specific heat capacity C_p can be obtained from the mass weight percentage of the specific heat capacities of the tissue components [22,23]:

$$C_p = \sum C_p^i w_i \tag{4}$$

where C_p^i is the specific heat capacity of a specified tissue component, and w_i is the mass fraction of a tissue component. The density ρ can be calculated as [22,23]:

#211182 - $15.00 USD Received 9 May 2014; revised 30 Jun 2014; accepted 7 Jul 2014; published 25 Jul 2014

$$\rho = \sum \rho^i w_i \tag{5}$$

where ρ^i is the density of the specified tissue component. From the density values at different temperatures, the volume change and thermal expansion coefficient can be estimated.

The estimated results of a typical beef muscle (Figs. 1(a) and 1(b)) show that thermal expansion coefficient and specific heat capacity are all temperature dependent parameters.

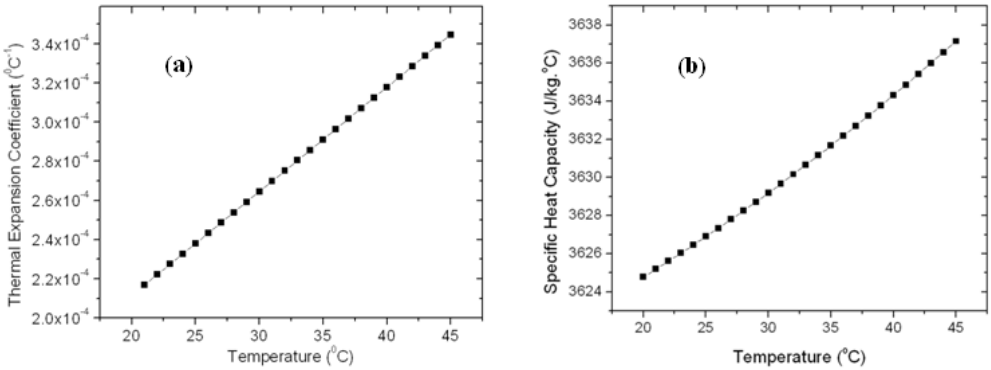

Fig. 1. (a) Estimated Thermal Expansion Coefficient of Beef Muscle as a Function of Temperature. (b) Estimated Specific Heat Capacity of Beef Muscle as a Function of Temperature.

Water plays an important role in bio-tissues. The total water content of the human skin is 65% and for abdominal muscles it is up to 77% [24]. The dependence of the Gruneisen parameter of water on temperature can be calculated as shown in Fig. 2(a) [25–27].

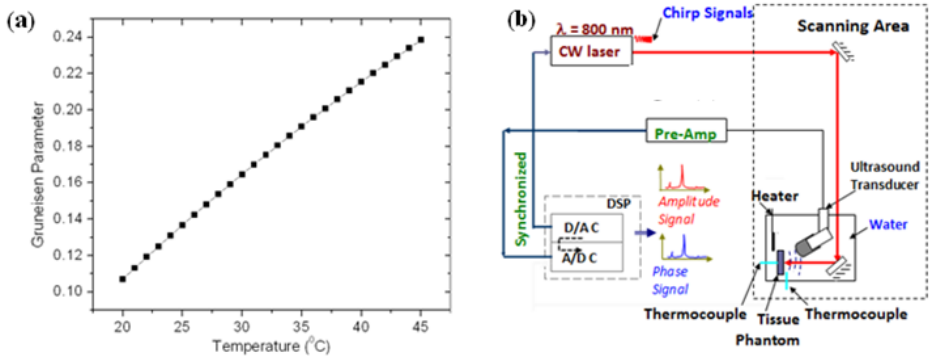

Fig. 2. (a) Gruneisen Parameter of Water Dependence on Temperature. (b) Experimental setup.

3. Experimental setup

The experimental setup diagram is shown in Fig. 2(b). A continuous wave (CW) diode laser emitting at 800 nm was used for experiments. The laser beam size was 3.5 mm. Linear frequency modulated (LFM) chirp signals (0.3 MHz to 1.3 MHz, 1 ms long) were generated by signal-generation card NI PXI-5421 (National Instrument, Austin, Texas), and utilized for laser modulation. A focused ultrasound transducer (Panametrics-NDT, V314 with −6dB range from 0.59 to 1.2 MHz, focal distance 1.9 inches) was employed as a detector of the photoacoustic signals. The detected signals were amplified by a pre-amplifier (Parametrics-NDT, 5676) first, and then were sent to the digital data-acquisition card NI PXIe-5122 (National Instrument, Austin, Texas). Two thermocouples (K type, Omega) were employed for temperature measurements.

#211182 - $15.00 USD Received 9 May 2014; revised 30 Jun 2014; accepted 7 Jul 2014; published 25 Jul 2014

Samples of ink solutions and *ex-vivo* beef muscle were prepared for experiments. The ink solutions were prepared by adding a small amount (about 1%) of liquid ink (Lamp black, Cotman) in distilled water, and the measured attenuation coefficient of the solutions was found to be 3.1 cm^{-1}. The *ex-vivo* beef muscle was purchased from a local market, and the samples were packed and kept at 2°C. The measured attenuation coefficient of *ex-vivo* beef muscle was 5.9 cm^{-1}.

4. Results and discussion

The speed-of-sound dependence on temperature was measured with two ultrasonic transducers: one worked as transmitter, and the other one played the role of receiver. The delay time of the signals and the distance between the two transducers were measured, thereby allowing the determination of the speed of sound in beef muscle. The measurement results are shown in Fig. 3(a). It is seen that the speed of sound in *ex-vivo* beef muscle c_{bf} increases from 1574.5 to 1593 m/s between 20 and 45°C.

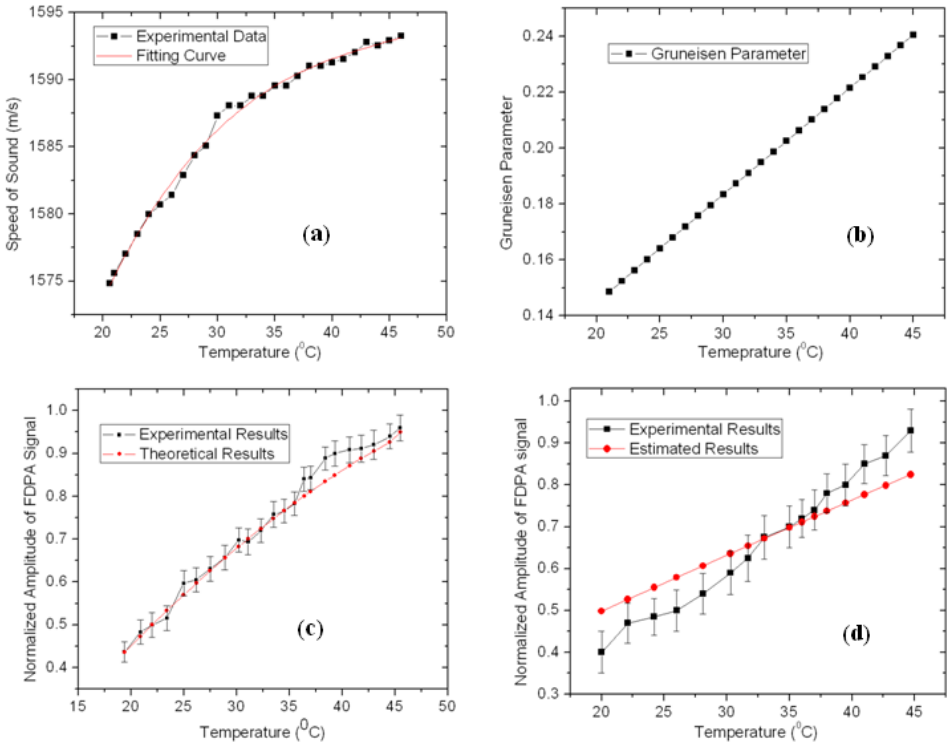

Fig. 3. (a) Speed of Sound of Beef Muscle Dependence on Temperature. (b) Estimated Gruneisen Parameter of Beef Muscle Dependence on Temperature. (c) PA Signal dependence on Temperature (Measured on ink solution, attenuation coefficient μ_{eff} = 3.1 cm^{-1}). (d) PA Signal dependence on Temperature (Measured on *ex-vivo* beef muscle, averaged attenuation coefficient μ_{eff} = 5.9 cm^{-1}).

From the previously estimated thermal expansion coefficient (Fig. 1(a)) and specific heat capacity (Fig. 1(b)), the Gruneisen parameter of beef muscle dependence on temperature was calculated as shown in Fig. 3(b). The Gruneisen parameter of beef muscle increases linearly between 22°C (0.15) and 37°C (0.21). The averaged experimental mean values and standard deviations of the temperature dependent PA radar signal are shown in Figs. 3(c) and 3(d) for the ink solution and beef muscle, respectively. It can be seen that the PA radar signals increase monotonically with rising temperature from 20 to 45°C. Theoretically estimated PA

#211182 - $15.00 USD Received 9 May 2014; revised 30 Jun 2014; accepted 7 Jul 2014; published 25 Jul 2014

radar (Eq. (1) results are also shown for comparison. There is a good correlation between the theory and experimental data for the ink solution. For the results with beef muscle, the PA data exhibit less, yet reasonable, agreement with the theoretically estimated values (Fig. 3(d)). The relative increases for ink solution and beef muscle are 112% and 135% from 20 to 45°C. These results are consistent with the findings from other research where the signal dependence on temperature was found using pulsed PA methods [13,14].

The attenuation coefficient dependence on temperature of the ink solution and the *ex-vivo* beef muscle was also studied. The results did not show any changes in the temperature range 20 to 45°C. This is in agreement with an earlier report [13]. The phase signals of the ink solution and beef muscle also did not exhibit any temperature dependence in the experimental results.

The experimental setup (shown in Fig. 4(a)) for studying imaging depth improvement with increased temperature consisted of a box filled with 0.47% intralipid solution as a scatterer [28]. The tested *ex-vivo* beef muscle samples were placed inside the box, and the box was moved by micrometer stages to simulate different absorber depths. In each case the foregoing heating experiment was repeated. Figure 4(b) shows the experimental results of the imaging depth study at various temperatures: Between 20 and 43°C the maximum imaging depth was doubled, and increased monotonically from 11 mm to 24 mm. At 37°C, the imaging depth was 19 mm, but increased to 22 mm at 41°C, and 24 mm at 43°C. The signal strength increase was about 91% from 20 to 37°C (13% from 37 to 43°C). The SNR increased by 52% from 20 to 43°C (8% from 37 to 43°C).

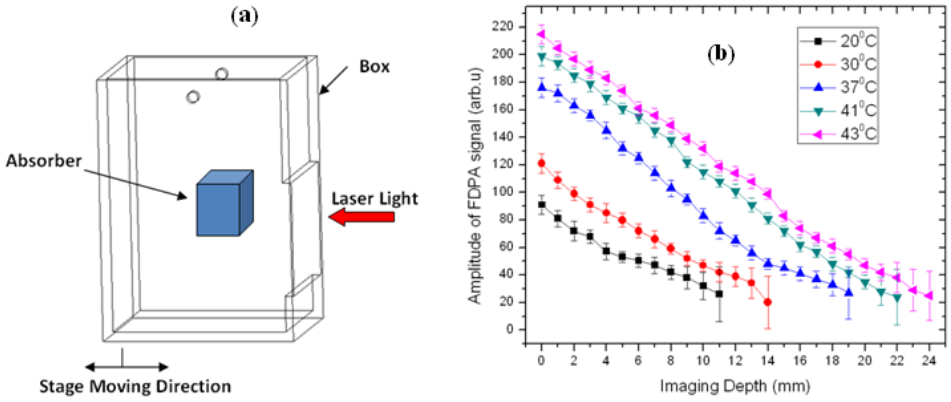

Fig. 4. (a) Experimental setup for PA radar imaging depth dependence on temperature. (b) PA radar signal dependence on temperature (measured on *ex-vivo* beef muscles).

5. Conclusions

A study of the temperature-dependent photoacoustic signal for depth improvement was undertaken. Experimental validation was performed using the PA radar modality. The speed of sound, thermal expansion coefficient and specific heat capacity were calculated theoretically and were found to be factors contributing to the increase of the Gruneisen parameter and the PA amplitude (the peak of cross-correlation) with temperature. The experimental results confirmed the theoretical temperature dependence of the Gruneisen parameter. The study showed that the thermally enhanced PA radar can increase the signal strength 13% and the imaging depth over 20% with a temperature increase from 37 to 43°C.

Acknowledgments

A. M. grateful for the support of NSERC through a Discovery Grant, and for the support of the Samsung Advanced Institute of Technology (SAIT) through a Global Research Outreach (GRO) Research Project Grant.

#211182 - $15.00 USD Received 9 May 2014; revised 30 Jun 2014; accepted 7 Jul 2014; published 25 Jul 2014